Allometric Models for Estimating Above- and Belowground Biomass for Coconut Palms in Tanzania

Wilson Ancelm Mugasha
wilson.mugasha@sua.ac.tz

Sokoine University of Agriculture
Eliakimu Zahabu
Sokoine University of Agriculture

Research Article

Keywords: Aboveground, belowground biomass, coconut, destructive sampling

Posted Date: December 19th, 2025

DOI: https://doi.org/10.21203/rs.3.rs-8347579/v1

Additional Declarations: No competing interests reported.

Version of Record: A version of this preprint was published at Agroforestry Systems on June 25th, 2026. See the published version at https://doi.org/10.1007/s10457-026-01559-8.

Abstract

This study developed the locally calibrated allometric models for estimating above- and belowground biomass (AGB and BGB) of coconut palms (*Cocos nucifera*) in Tanzania as a function of diameter at breast height (D) and total height (H). Destructive sampling was conducted on 46 palms for AGB and 29 palms for BGB across two contrasting coastal districts: Mkuranga, located along the Indian Ocean, and Kisarawe, situated farther inland. Five nonlinear model forms were fitted for to both pools, and model performance was assessed using R^2, RMSE, AIC, and Mean Prediction Error (PE%). Leave-one-out cross-validation (LOOCV) was applied to evaluate predictive reliability given the limited sample size. Model results showed moderate explanatory power, with R^2 ranging from 0.62–0.75 for AGB and 0.52–0.53 for BGB. Contrary to conventional findings for dicotyledonous trees, H consistently outperformed D as the strongest predictor for both AGB and BGB. This pattern reflects the monocot growth form of coconut palms, where D stabilizes early while biomass accumulates primarily through vertical growth. Models combining H and D did not significantly improve predictive accuracy and often produced insignificant coefficients. LOOCV confirmed that H-only models yielded the lowest bias and most consistent predictive performance. The study provides the allometric equations for coconut palms in Tanzania, offering an essential tool for biomass quantification in coconut-based agroforestry systems and carbon accounting frameworks. These models represent a methodological advance over generic IPCC defaults and support a more accurate assessment of carbon stocks in coastal agricultural landscapes.

1. Introduction

Coconut (*Cocos nucifera*) is among the four major palm species of economic importance among nearly 2400 palm species in the world. The other three palm with economic importance are *Elaeis oleifera, Borassus flabellifer* and *Phoenix dactylifera* (Arancon 1997; Goodman et al. 2013; Govaerts et al. 2005). The majority of coconut are found in higher rainfall coastal areas characterized by saline soils (Kant 2010). In Tanzania mainland, coconut trees are dominantly found in regions located in the eastern coast and quite few in patches in non-coastal regions. In the end of 1990s, the number of coconut trees in Tanzania was estimated to be about 22.6 million, growing on 240,000 ha where about 95% of the coconut acreage was grown by smallholder farmers (Mwinjaka et al. 1999).

Coconut trees are highly valued multipurpose species in the tropics, supporting rural livelihoods and contributing to ecological stability. Their various components, i.e., fruits, fronds, trunk wood, husk fibres and sap, provide multiple income sources and essential household goods such as food, beverages, fuel and construction materials, thereby strengthening livelihood resilience (Durst et al. 2004; Kumar and Kunhamu 2022). The coconut fruit is the most widely produced and commercially important nut globally, contributing significantly to international trade through products like coconut oil, desiccated coconut, coconut milk, coir fibre and activated charcoal, which sustain agro-industries across Asia, Africa and the Pacific (DebMandal and Mandal 2011).

On the other hand, coconut is widely integrated into agroforestry systems due to its favourable ecological and structural characteristics. Research indicates that monocropped coconut plantations use only about

22% of the land area, with canopy cover of roughly 30% and effective capture of around 45% of incoming solar radiation. Coconut palms also enhance soil conditions by increasing available phosphorus, improving exchangeable potassium, and conserving soil moisture (Senarathne and Udumann 2019). Consequently, intercropping coconut with various annual and perennial crops is a common strategy across coconut-growing regions to improve land-use efficiency and overall productivity (Nayak et al. 2025). Depending on palm age and spacing, which influence the amount of light reaching the understory, coconut-based systems can support a wide range of shade-sensitive, shade-intolerant, shade-tolerant, and shade-loving crops. More than 100 different crops and cropping systems have been documented as compatible intercrops within coconut plantations (Atapattu and Udumann 2025; Kumar and Kunhamu 2022).

In Tanzania, coconut cultivation is a major agricultural activity, particularly along the eastern and southern coastal zones, including the Pwani, Lindi, and Mtwara regions, where favourable climatic and soil conditions support its growth. The total area under coconut production was estimated at approximately 265,049 hectares in 2012 (Muyengi et al. 2015). Smallholder farmers dominate the sector, contributing the bulk of national production. According to the National Bureau of Statistics, coconut farming plays a critical economic role along the coastal belt, where an estimated 75% of household income for coconut-growing farmers is derived from the crop (NBS 2012).

Nevertheless, the potential of coconut palms to sequester atmospheric carbon dioxide remains another underutilised avenue for smallholder coconut farmers. As a long-lived perennial with continuous biomass accumulation, coconut palms can store carbon in their trunks, fronds, roots, and harvested products. Given its widespread cultivation, coconut-based agroforestry systems are viable candidates for carbon projects, particularly those aligned with Afforestation, Reforestation, and Revegetation (ARR) methodologies. By integrating coconut cultivation into certified carbon schemes, smallholders could gain additional income through carbon credits while contributing to climate change mitigation and promoting more sustainable land management practices (Ranasinghe and Thimothias 2012; Roupsard et al. 2002). An added advantage of coconut trees to the farmers is that few other woody vegetation types grow in coastal saline lands (Atapattu and Udumann 2025). Therefore, coconut trees present a strong opportunity for communities in coconut-growing regions to benefit from carbon market initiatives. Estimates indicate that mature coconut palms can store approximately 31.69 t C ha^{-1} on average (Namitha et al. 2025; Pragasan and Kalaiselvi 2024), while their annual carbon sequestration potential is around 2.63 t C ha^{-1} (Boomiraj et al. 2020). These values highlight the substantial climate-mitigation role of coconut-based systems and their suitability for participation in carbon projects, particularly those targeting long-term biomass accumulation.

However, accurate estimation of carbon stored in coconut palms requires reliable biomass allometric equations, which are currently lacking in Tanzania. Coconut palms differ fundamentally from dicotyledonous trees in their morphology, biomass allocation, and growth dynamics, rendering dicot-based allometric models unsuitable for palms. Moreover, biomass accumulation in coconut varies across ecological conditions such as soil salinity, rainfall, and management regimes, highlighting the need for site-specific calibration. The absence of such models currently limits the precision of carbon stock assessments and represents a major barrier to the development of credible coconut carbon projects (IPCC 2006). Most of the biomass allometric models developed focused on the dicotyledon trees (e.g., Masota et al. 2016; Mugasha et al. 2013). On the other hand, Goodman et al. (2013) developed biomass allometric models for nine palm species. However, their work did not include the coconut palm, leaving a significant research gap for this economically important species. Additionally, to authors' knowledge, there are limited published studies that have established allometric models for belowground biomass of coconut palms, despite the substantial contribution of root biomass to total carbon stocks. Against this background, this study aimed to develop allometric models for above- and belowground biomass of coconut palms growing in Tanzania.

2. Methods and materials

2.1. Study site description

This study was conducted in the Mkuranga and Kisarawe districts of the Pwani Region. Mkuranga lies approximately 50 km south of Dar es Salaam, bordering the Indian Ocean coastline, whereas Kisarawe is situated about 78 km inland from the coast. Mkuranga district is located at longitudes 39^{o} 09" 16' E and latitudes of 07^{o} 17" 23' S while Kisarawe is located at longitudes of 38^{o} 44" 12' E and latitudes of 07^{o} 15" 44' S. both districts are found below 500 m above sea level. The mean annual temperature and rainfall is 28^{0}C and 1090 mm, respectively (Muyengi et al. 2015).

The soils are dominated by sandy and fluvisol soils. The vegetation in both districts in Tanzania is characterised by a diverse range of ecosystems, influenced by both natural and anthropogenic factors. The settlements and agricultural farms adjacent to natural vegetation in the study districts exhibit a variety of vegetation types, from savannahs to forests, each with unique species compositions and ecological dynamics (Minja 2006).

2.2. Study design

Mixed-age coconut farms belonging to different household owners were selected as sampling sites for data collection. These farms included both pure coconut monocultures and coconut palms integrated into agroforestry systems, where they are intercropped with various annual and perennial crops. In the study areas, farm sizes are generally small, irregularly shaped, and spatially fragmented. This landscape structure constrained the establishment of systematic sample plots that would normally support random selection of sampling units.

Consequently, a purposive sampling approach was adopted to ensure adequate representation of the full structural variability within the coconut population. Sample palms were deliberately chosen to capture a broad range of age classes and morphological characteristics, particularly total height (H) and diameter at breast height (D), as summarised in Table 1. At each study site, 23 coconut palms were selected for destructive sampling, ensuring sufficient coverage of the size distribution needed for robust allometric model development.

2.3. Data collection

2.3.1. Measurement of single palm parameters

Prior to destructive sampling, the coconut trees were measured for D using calliper and H excluding rachis using Suunto hypsometer. The H was measured at the bottom of the youngest rachis (Fig. 2). Summary statistics of sampled coconut trees are presented in Table 1. It is important to note that it was not possible to include young coconut trees whose trunks were still occupied by rachis below 1.3 m from the ground. As a result, the minimum D was 19.0 cm.

2.3.2. Destructive sampling and determination of biomass

The aboveground component consists of the stem, rachis, fruits and leaflets (Fig. 2). The stem was further divided into two parts: the hard (lower) and soft (upper) sections. The hard parts are often used to produce timber and charcoal. The separation was important to ensure that moisture variation across the stem is well captured, i.e., parts with a relatively similar moisture content are grouped together. After separating the major biomass components, each section was crosscut into billets approximately 1 m in length to facilitate handling and accurate weighing. Every billet was weighed immediately in the field, and its green (fresh) weight was recorded. For the foliage component, leaflets were carefully removed from the rachis, bundled together, and their fresh weight measured separately. The rachis portions were similarly bundled and weighed to obtain their green weight. For each primary biomass component, namely the stem (both hard and soft tissues), leaves, fruits, and rachis, three representative sub-samples were collected to capture within-component moisture variability. Each sub-sample was clearly labelled, and its green weight recorded, ready for laboratory analysis. These sub-samples served as the basis for determining moisture content and developing fresh-to-dry biomass conversion factors required for biomass estimation.

The belowground component consists of two main parts: the root collar and the roots (Fig. 3). Due to the fibrous nature of coconut tree roots, BGB was determined by excavating an area of 1.5 m radius from the coconut tree to a depth of 1.5 m. This is because most of the coconut tree roots are within this radius and depth (Thampan 1981). The coconut trees were excavated while standing, so they would fall under their own weight and consequently uproot most of the fibrous roots. The remaining roots were excavated around the prescribed area. Roots were removed from the root crown and then both root crown and roots were cleaned for soil and measured for fresh weight. For each of the two belowground components, at least three sub-samples were collected and fresh weighed for laboratory analysis. In the laboratory, the collected sub-samples were oven dried at 105 ± 2 ^{o}C for at least 72 hours until they attained a constant weight.

2.3.3. Laboratory procedures

The sub-samples of each biomass component were taken to the laboratory for drying at a temperature of 107°C. The drying process took at least 72 hours to reach constant weight depending on the sample component and species. The wood samples were placed in the oven while they were in the paper bag. This is because, as wood samples dry, they tend to disintegrate. The weighing process was repeated every six hours until the samples reached a constant weight, indicating that they are completely dry.

2.3.4. Estimating the above and below ground dry weight (biomass)

Fresh and over-dry weight of each sub-sample was used to establish the relationship between dry weight and green weight using Eq. 1.

$$R = \raisebox{1ex}{DR}/\raisebox{-1ex}{GW} \times 100$$

1

Where *R* is the ratio dry weight to green weight in %; DR is the dry weight; and GW is the fresh or green weight.

The average R value for each main above and below sub-component (soft stem, hard stem, leaves, rachis, root collar, and roots) was subsequently calculated. The average R value was employed to convert the green weight of each component to dry weight by multiplying the green weight by R. The summation of the dry weight of all tree components provided the total tree AGB and BGB. Description statistics of the prepared data for AGB and BGB modelling are presented in Table 1.

Table 1
Summary statistics of the sample tree used for developing below and above ground models

Component	**Site**	**n**	**D (cm)**			**H (m)**		
			Mean	**Min.**	**Max.**	**Mean**	**Min.**	**Max.**
AGB	Mkuranga	23	29.4	21.0	40.0	8.1	1.6	14.4
	Kisarawe	23	29.5	19.0	39.0	12.7	5.9	21.0
	All	46	29.5	19.0	40.0	9.9	1.6	21.0
BGB	Mkuranga	14	29.7	21.0	37.0	8.4	1.6	14.4
	Kisarawe	15	29.3	22.5	38.0	12.2	9.6	15.3
	All	29	29.5	21.0	38.0	9.5	1.6	15.3

2.3.5. Model fitting and evaluation

Biomass and volume data were fitted to non-linear functions (1–4), which are commonly used and widely documented in the literature (Chave et al. 2014; Zianis et al. 2005). A maximum likelihood modelling approach was applied using PROC NLP, a procedure in SAS (SAS®, 2008). In addition, the procedure accounts for heteroscedasticity by modelling the variance in the form of: $a0 \times \mathrm{D}^{a1}$ where $a0$ and $a1$ are parameters to be estimated.

$$AGB = a_0 \times H^{a_1}$$

1

$$AGB = a_0 \times D^{a_1}$$

2

$$AGB = a_0 \times D^{a_1} \times H^{a_2}$$

3

$$AGB = a_0 \times (D^2 \times H)^{a_1}$$

4

$$AGB = a_0 + a_1 \times D + a_2 \times H$$

5

Where Y is the dependent variable, i.e., AGB and BGB in kg; a, b and c are unknown parameters to be estimated; H and D are the total height and diameter at breast height, respectively.

For each fitted equation, Root Mean Square Error (RMSE) and R2 were computed using equations 5 and 6, respectively. The Mean Prediction Error (PE%) and Akaike information criterion (AIC) were computed using equations 7 and 8, respectively. The selection of the best-performing models was based on low AIC and PE%. Other model performance criteria, such as RMSE and $R^{2,}$ were presented to show the quality of the developed models.

$$SE = \sqrt{\frac{\sum_{i=1}^{n}(B_i - \widehat{B}_i)^2}{n}}$$

5

$$R^2 = 1 - \left(\frac{\sum (B_i - \widehat{B}_i)^2}{\sum (B_i - \bar{B})^2}\right)$$

6

$$PE\% = \backslash\text{raisebox}1ex\$100\$/\backslash\text{raisebox}-1ex\$n\$ \times \sum_{i=1}^{n}\left(\frac{B_i - \widehat{B}_i}{B_i}\right)$$

7

$$AIC = 2k - 2l$$

8

Where B_i and $\widehat{B}_i$ are observed and estimated ABG or BGB of trees for observation i; *n* is the number of *observations*; *k* is the number of all the estimated model parameters, and l is the value of the log-likelihood.

2.3.6. Model evaluation

The selected model was evaluated using leave-one-out cross-validation (LOOCV), a robust validation technique well-suited to datasets with small sample sizes (Cheng et al. 2021; Stephenson and Broderick 2020). In LOOCV, each observation is iteratively excluded from the dataset, the model is refitted using the remaining observations, and the excluded observation is then predicted. The PE% is then computed for the excluded observation. In addition, the mean SE% (Eq. 9) was computed across all iterations. The overall PE% was computed as the mean of the PE% values across iterations. This process is repeated until every observation has served as the validation point once. In this study, conventional data-splitting approaches, such as partitioning the dataset into independent training and validation subsets, were not feasible due to the limited number of observations: only 46 for AGB and 29 for BGB. Creating separate subsets from such small samples would have reduced model stability, weakened parameter estimation, and compromised the reliability of the validation results.

$$SE\% = 100 \times \left(\sqrt{\frac{\sum_{i=1}^{n} (B_i - \widehat{B}_i)^2}{n}} \Big/ \bar{B} \right) \tag{9}$$

Where SE% is the percentage standard error relative to the mean value of AGB or BGB, B_i and $\widehat{B}_i$ are observed and estimated ABG or BGB of trees for observation i, $\bar{B}$ is the mean value of observed ABG or BGB.

3. Results

3.1. Model performance

The performance of the AGB and BGB models is summarised in Table 2. For AGB, the R^2 ranged from 0.62 to 0.75, while for BGB it ranged from 0.52 to 0.53. Similarly, the SE ranged from 85 to 101 for AGB and from 15.61 to 15.75 for BGB. Notably, and contrary to expectations, increasing the number of explanatory variables did not consistently improve model performance, as measured by R^2 or SE. The pattern of PE% further supports this observation. PE% tended to increase as more explanatory variables were added, ranging from 4.49% to 15.62% for AGB and from 9.26% to 11.63% for BGB. In addition, Model 4 (AGB) and Models 3 and 5 (BGB), all of which combined H and D, exhibited comparatively low and statistically insignificant PE% values. Additionally, most models that incorporated both H and D produced insignificant coefficient estimates, except for Model 5 for AGB.

The best performing model was the model that included only H (Model 1) for both AGB and BGB. Adding D to the models did not improve model fit. This is contrary to expectations, where D often shows a stronger correlation with AGB and BGB than H does. Therefore, model 1 was selected for further evaluation. The model's expressions for the selected models for ABG and BGB are presented in equations 10 and 11, respectively. The model residual plots are presented in Fig. 6 and Fig. 7 for the AGB and BGB models, which had no insignificant coefficients. The residual plots did not show any pattern that indicated the models' bias.

Table 2
Performance of aboveground and belowground biomass models

Component	Model number	Model Expression	R^2	SE	PE%	AIC
Aboveground	1	$AGB = a_0 \times H^{a_1}$	0.75	88.49	-5.02	543.86
	2	$AGB = a_0 \times D^{a_1}$	0.73	85.11	-0.62	551.82
	3	$AGB^{**} = a_0 \times D^{a_1} \times H^{a_2}$	0.72	86.77	-4.29	552.23
	4	$AGB^{**} = a_0 \times (D^2 \times H)^{a_1}$	0.62	101.02	-15.62*	556.23
	5	$AGB = a_0 + a_1 \times D + a_2 \times H$	0.70	89.90	-8.06	547.96
Belowground	1	$AGB = a_0 \times H^{a_1}$	0.53	15.70	-9.26	252.24
	2	$AGB = a_0 \times D^{a_1}$	0.52	15.62	-9.01	255.71
	3	$AGB^{**} = a_0 \times D^{a_1} \times H^{a_2}$	0.53	15.57	-10.71*	263.53
	5	$AGB^{**} = a_0 + a_1 \times D + a_2 \times H$	0.52	15.75	-11.63*	264.18
*The value of PE% was significantly different from zero (*p* > 0.05)						

The root/shoot (RS) ratio ranged from 0.1 to 0.42 with mean value of 0.24. The findings show the RS ratio decreased linearly with the increase of D and H (Fig. 5).

3.2. Validation of the selected models

The validation results (Table 3) indicate that models using H alone as the predictor generally provide the most reliable estimates of both AGB and BGB, outperforming models based solely on D, except for the AGB model incorporating both D and H. The H-only models exhibit lower PE% values (AGB = -9.7%; BGB = -10.80%) and SE% values (AGB = 48.3%; BGB = 34.54%), demonstrating reduced bias and greater precision. Although AGB model combining all the variables (D & H) produces the lowest PE% (-6.12%), it is accompanied by a higher SE% (49%), indicating greater variability in predictions. Overall, the confidence intervals around the mean values of PE% and SE% increase when moving from H-only models to those using D alone or a combination of H and D, highlighting the stronger predictive performance of H-only models. Based on these findings, models with only H were finally selected for both ABG and BGB and one additional model for predicting AGB that includes both H and D (models 10, 11, and 12).

Table 3
Validation results

Component	Model Expression	PE%	SE%
Aboveground	$AGB = a_0 \times H^{a_1}$	-9.08 ± 12.24	48.3 ± 12.78
	$AGB = a_0 \times D^{a_1}$	-28.41* ± 11.99	48.46 ± 12.57
	$AGB = a_0 + a_1 \times D + a_2 \times H$	-6.12 ± 11.99	49.16 ± 12.74
Belowground	$AGB = a_0 \times H^{a_1}$	-10.80 ± 16.43	34.54 ± 11.74
	$AGB = a_0 \times D^{a_1}$	-20.79 ± 23.81	44.26 ± 15.59

$$AGB = 19.7012 \times \ H^{1.14383}$$

10

$$AGB = \ -228.9568 + 8.7556 \times \ D + 25.1578 \times \ H$$

11

$$BGB = 10.9418 \times \ H^{0.75856}$$

12

4. Discussion

Data for developing the AGB and BGB models was collected from two districts, Kisarawe and Mkuranga. These sites were deliberately selected to capture the range of environmental conditions under which coconut palms grow within the coastal zone. Mkuranga is situated adjacent to the Indian Ocean shoreline, experiencing direct coastal influence, including higher humidity, saline winds, and moderated temperatures. In contrast, Kisarawe is located farther inland, where coconut palms grow under comparatively drier and less saline conditions. This ecological gradient provides a useful basis for assessing how differences in site characteristics may influence the accumulation of AGB and BGB across sites (e.g., Santos et al. 2020).

The developed models had R^2 ranging from 0.62 to 0.75 for AGB and from 0.52 to 0.53 for the BGB. These values are relatively low compared to many allometric models developed for dicotyledonous tree species, which often report R^2 values of at least 0.80 (Chave et al. 2014; Mugasha et al. 2016; Mwakalukwa et al. 2014). The lower coefficients of determination observed in this study suggest a high degree of variability among coconut palms, highlighting the need for larger datasets to better capture this variation. For example, allometric models developed for miombo woodlands, where a minimum of 40 trees per site were used across Lindi, Babati, Tabora, and Mpanda, achieved R^2 values of at least 0.80 for AGB when using D and D as predictors (Mugasha et al. 2013). Given the multispecies composition and structural heterogeneity typical of miombo ecosystems, one would expect lower R^2 values in such contexts compared to single-species models like coconut palms. The relatively lower R^2 observed in the present study, therefore, underscores the complexity and variability inherent in coconut biomass allocation.

Conversely, the results indicated that H was a stronger predictor of both AGB and BGB. This contrasts with the findings of most biomass allometry studies, which typically identify D as the most powerful predictor (Altanzagas et al. 2019; Chave et al. 2005; Huy et al. 2016; Kuyah et al. 2012) but in agreement with other studies developed the biomass allometric equations for different types of palm genus (e.g., Goodman et al. 2013). This deviation is likely linked to the unique morphology of coconut palms. At younger ages, palms tend to exhibit relatively large D despite having comparatively low AGB and BGB. As the palms mature, D does not consistently increase in parallel with biomass accumulation (Fig. 4). This pattern reflects the monocot growth form of coconut palms, which lack secondary diameter growth, causing D to stabilize early while biomass continues to accumulate resulting weak AGB and BGB predictive power of D (e.g., Tomlinson 1990). Similar finding have been reported elsewhere on the strength of stem H in describing the variation of AGB and BGB for oil (Sanquetta et al. 2015). This highlights the importance of species-specific or growth-form-specific allometric models rather than relying on generalized equations derived from dicot species.

The LOOCV results showed distinct patterns in prediction performance across the different model structures. For AGB, the mean PE% increased when moving from the model that used only H to the model that relied solely on diameter D. Despite this increase, the confidence intervals around the mean PE% remained relatively stable across all variable combinations, suggesting a consistent level of variability in PE% among the models. When both H and D were included simultaneously, the AGB model's PE% improved substantially. For BGB, the model with only H had better fit while model with only D produced larger D. Models with both H and D produced insignificant coefficients and therefore, they were not considered in the validation. However, the improvement in PE% came with a trade-off. The model incorporating all variables exhibited slightly higher SE% compared with the model using only H. This increase in SE% implies that, although the combined model reduced systematic bias, it introduced a greater degree of uncertainty around the PE% (Chave et al. 2014). Such a pattern suggests that adding predictor variables may enhance accuracy but can also increase model complexity and which may result to overfitting and perform poorly when prediction the biomass of new observations. Understanding this balance between bias reduction and uncertainty is critical when selecting the most appropriate model for biomass estimation (Cosenza et al. 2025; Silva et al. 2013).

Overall, the validation results indicate that, despite being identified as the best-performing model for BGB, its predictive power remained relatively weak. This limitation is most likely attributable to the high inherent variability in belowground biomass and the relatively small sample size used for model development. As is common in biomass studies, researchers face a trade-off between obtaining a sufficiently large number of observations, an approach that improves model reliability but substantially increases cost and labour, and relying on fewer observations, which reduces cost but compromises the precision and robustness of the resulting model. In this study, the intensive labour and technical effort required to excavate and measure BGB restricted data collection to only 29 observations, which likely contributed to the observed level of uncertainty and reduced predictive accuracy (e.g., Kuyah et al. 2012). Nevertheless, the current model for BGB and the provided pattern of RS provide reliable BGB estimate as compared to the default value provided by IPCC (IPCC 2006).

The developed allometric models for estimating AGB and BGB provide a practical and locally calibrated tool for estimating AGB and BGB of coconut palms in Tanzania. Their application is particularly relevant for biomass accounting in smallholder coconut-based farming systems, carbon stock assessments, and monitoring activities under emerging carbon projects. Since H emerged as the strongest and most consistent predictor of both AGB and BGB, the selected models are especially suitable for rapid field assessments where measuring D is challenging or provides little additional predictive value for palms. When applied within the size range represented in this study (D: 19–40 cm; H: 1.6–21 m), the models offer reliable biomass estimates and represent an improvement over default biomass factors such as those provided in the IPCC Guidelines. For programs such as ARR-based carbon initiatives, or farm-level carbon appraisals, these models facilitate more accurate and cost-effective quantification of coconut biomass and associated carbon stocks. However, users should ensure that model deployment remains within the ecological and size conditions of the calibration dataset and, where possible, validate the equations with additional field observations from new sites to support broader regional application.

5. Conclusion

This study presents the first locally calibrated allometric models for estimating AGB and BGB of coconut palms in Tanzania, with H emerging as the strongest predictor due to the species' monocot growth form. Although model performance was moderate, the equations offer a substantial improvement over generic default values and provide a reliable basis for biomass and carbon stock estimation in coastal agroforestry systems. Validation results confirmed that H-only models yield the most robust and least biased predictions, underscoring the importance of accurate H measurement during field application. Given the limited sample size, particularly for BGB, future efforts should expand destructive sampling across broader ecological gradients to refine and validate these models. Adoption of these equations in carbon accounting frameworks and further independent testing across coconut-growing regions in Tanzania and East Africa will enhance confidence in their wider application and support more accurate assessment of the carbon sequestration potential of coconut-based land-use systems.

Declarations

Competing interests:

The authors declare no competing interests

Funding:

The field work was funded through the project “*Development of biomass estimation models and carbon monitoring in selected vegetation types of Tanzania*” under the Climate Change Impacts, Adaptation and Mitigation (CCIAM) programme in Tanzania.

Author Contribution

WAM and EZ jointly designed the study and collected the data. WAM conducted the data analysis and prepared the first draft of the manuscript. EZ provided substantial contributions to the revision and refinement of the manuscript.

Acknowledgement

The author gratefully acknowledges the support provided by the District Councils, whose assistance was instrumental in facilitating this study. Sincere appreciation is also extended to the farmers who granted access to their coconut palms and farms, without whom the field data collection would not have been possible.

Data Availability

The data used in this study will be made available upon request.

References

1. Altanzagas B, Luo Y, Altansukh B, Dorjsuren C, Fang J, Hu H (2019) Allometric equations for estimating the above-ground biomass of five forest tree species in Khangai, Mongolia. Forests 10:661
2. Arancon RN (1997) Asia Pacific forestry sector outlook: focus on coconut wood. Asia-Pacific Forestry Towards 2010. Asia-Pacific For. Sect. Outlook Study Work. Pap. Ser.
3. Atapattu AJ, Udumann SS (2025) Leveraging agroforestry principles for nature-based climate-smart solutions for coconut cultivation. In: Handb. nature-based Solut. to Mitig. Adapt. to Clim. Chang. Springer, pp 1931–1958
4. Boomiraj K, Jagadeeswaran R, Karthik S, Poornima R, Jothimani S, Sudhagar RJ (2020) Assessing the carbon sequestration potential of coconut plantation in Vellore district of Tamil Nadu, India. Int J Environ Clim Chang 10:618–624

5. Chave J, Andalo C, Brown S, et al (2005) Tree allometry and improved estimation of carbon stocks and balance in tropical forests. Oecologia 145:87–99
6. Chave J, Réjou-Méchain M, Búrquez A, et al (2014) Improved allometric models to estimate the aboveground biomass of tropical trees. Glob Chang Biol. https://doi.org/10.1111/gcb.12629
7. Cheng J, Dekkers JCM, Fernando RL (2021) Cross-validation of best linear unbiased predictions of breeding values using an efficient leave-one-out strategy. J Anim Breed Genet 138:519–527
8. Cosenza DN, Saarela S, Strunk J, Korhonen L, Maltamo M, Packalen P (2025) Effects of model-overfit on model-assisted forest inventory in boreal forests with remote sensing data. For An Int J For Res 98:507–521
9. DebMandal M, Mandal S (2011) Coconut (Cocos nucifera L.: Arecaceae): in health promotion and disease prevention. Asian Pac J Trop Med 4:241–247
10. Durst PB, Killmann W, Brown C (2004) Asia's new woods. J For 102:46–53
11. Goodman RC, Phillips OL, del Castillo Torres D, Freitas L, Cortese ST, Monteagudo A, Baker TR (2013) Amazon palm biomass and allometry. For Ecol Manage 310:994–1004
12. Govaerts R, Dransfield J, Dransfield J (2005) World checklist of palms: Royal Botanic Gardens. Deurne MIM 2:66
13. Huy B, Kralicek K, Poudel KP, Phuong VT, Van Khoa P, Hung ND, Temesgen H (2016) Allometric equations for estimating tree aboveground biomass in evergreen broadleaf forests of Viet Nam. For Ecol Manage 382:193–205
14. IPCC (2006) 2006 IPCC guidelines for national greenhouse gas inventories. Inst. Glob. Environ. Strateg. Hayama, Kanagawa, Japan
15. Kant P (2010) Should bamboos and palms be included in CDM forestry projects (No. 07). IGREC Working Paper No. IGREC07: 2010
16. Kumar BM, Kunhamu TK (2022) Nature-based solutions in agriculture: A review of the coconut (Cocos nucifera L.)-based farming systems in Kerala,"the Land of Coconut Trees." Nature-Based Solut 2:100012
17. Kuyah S, Dietz J, Muthuri C, Jamnadass R, Mwangi P, Coe R, Neufeldt H (2012) Allometric equations for estimating biomass in agricultural landscapes: II. Belowground biomass. Agric Ecosyst Environ 158:225–234
18. Masota AM, Bollandsås OM, Zahabu E, Eid T (2016). Allometric biomass and volume models for lowland and humid montane forests. Allometric Tree Biomass Vol Model Tanzania 35
19. Minja M (2006) The state of tree cutting and charcoal burning in Mkuranga district. Dar es Salaam. 73pp.
20. Mugasha WA, Bollandsås OM, Eid T (2013) Relationships between diameter and height of trees in natural tropical forest in Tanzania. South For. https://doi.org/10.2989/20702620.2013.824672
21. Mugasha WA, Eid T, Bollandsås O, Malimbwi R, Chamshama S, Zahabu E, Katani J (2013) Allometric models for prediction of above- and belowground biomass of trees in the miombo woodlands of Tanzania. For Ecol Manage. https://doi.org/10.1016/j.foreco.2013.08.003

22. Mugasha WA, Mwakalukwa EE, Luoga E, Malimbwi RE, Zahabu E, Silayo DS, Sola G, Crete P, Henry M, Kashindye A (2016) Allometric Models for Estimating Tree Volume and Aboveground Biomass in Lowland Forests of Tanzania. Int J For Res. https://doi.org/10.1155/2016/8076271
23. Muyengi ZE, Msuya E, Lazaro E (2015) Assessment of factors affecting coconut production in Tanzania. J Agric Econ Dev 4:083–094
24. Mwakalukwa EE, Meilby H, Treue T (2014) Volume and aboveground biomass models for dry miombo woodland in Tanzania. Int J For Res 2014:531256
25. Mwinjaka S, Chiduza C, Temu A, Sukume C, Diehl L (1999) Cocunut palm replacement model for Tanzanian farming systems. J Agric Econ Dev 3:61–70
26. Namitha V V, Raj SK, Prathapan K (2025) Carbon Sequestration Potential in Coconut based Cropping System: A Review. Agric. Rev. 46:
27. Nayak S, Davis PL, Ajithkumar B, Vysakh A (2025) Optimizing Carbon Sequestration: The Role of Coconut Palm in Agroforestry. Int J Environ Clim Chang 15:242–255
28. NBS (2012) Livestock Sector National Report Census of Agriculture 2007/2008. National Bureau Statistics. Dar es Salaam
29. Pragasan LA, Kalaiselvi M (2024) Carbon Stock Potential of Coconut Plantations in University Campus: A Case Study from Coimbatore, India. Asian J Res Agric For 10:140–146
30. Ranasinghe CS, Thimothias KSH (2012) Estimation of carbon sequestration potential in coconut plantations under different agro-ecological regions and land suitability classes. J. Natl. Sci. Found. Sri Lanka 40:
31. Roupsard O, Bonnefond J-M, Jourdan C, Epron D, Irvine MR, Berbigier P, Nouvellon Y, Joffre R, Taga S, Sileye T (2002) Carbon sequestration by Coconut plantations in Oceania (Vanuatu).
32. Sanquetta CR, Sylvio PÃ, Dalla Corte AP, Behlin A, Sanquetta MNI (2015) Quantifying biomass and carbon stocks in oil palm (Elaeis guineensis Jacq.) in Northeastern Brazil. African J Agric Res 10:4067–4075
33. Santos MMS, Lacerda CF, Neves ALR, de Sousa CHC, de Albuquerque Ribeiro A, Bezerra MA, da Silva Araújo IC, Gheyi HR (2020) Ecophysiology of the tall coconut growing under different coastal areas of northeastern Brazil. Agric Water Manag 232:106047
34. Senarathne SHS, Udumann SS (2019) Evaluation of coconut based Anacardium occidentale agroforestry system to improve the soil properties of coconut growing lands in wet, intermediate and dry zone of Sri Lanka. Cord 35:1–10
35. Silva S, Ingalalli V, Vinga S, Carreiras JMB, Melo JB, Castelli M, Vanneschi L, Gonçalves I, Caldas J (2013) Prediction of forest aboveground biomass: an exercise on avoiding overfitting. In: Eur. Conf. Appl. Evol. Comput. Springer, pp 407–417
36. Stephenson W, Broderick T (2020) Approximate cross-validation in high dimensions with guarantees. In: Int. Conf. Artif. Intell. Stat. PMLR, pp 2424–2434
37. Thampan PK (1981) Handbook on coconut palm.
38. Tomlinson PB (1990) The structural biology of palms. Oxford University Press

39. Zianis D, Muukkonen P, Mäkipää R, Mencuccini M (2005) Biomass and stem volume equations for tree species in Europe.

Figures

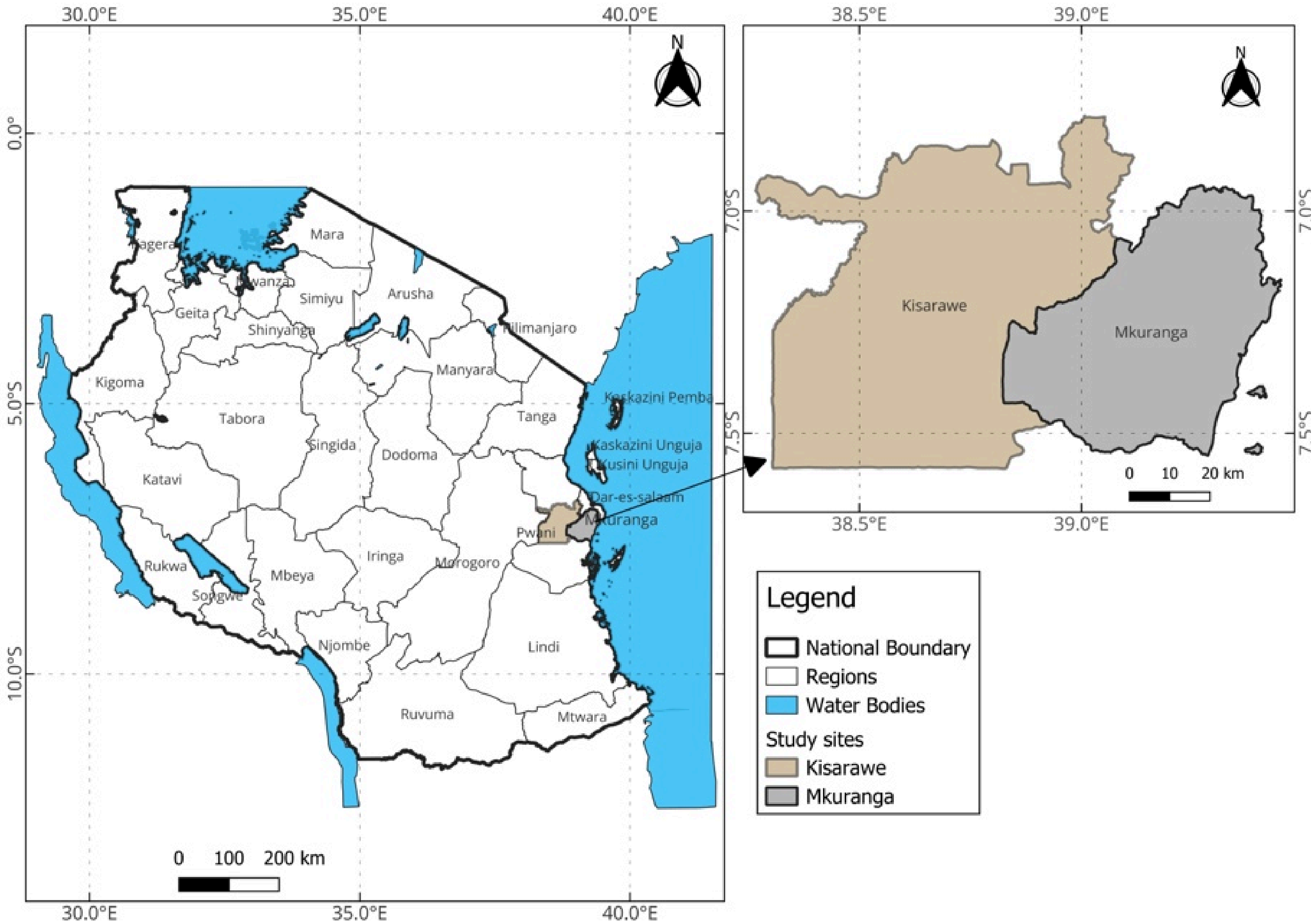

Figure 1

Map showing the studied districts

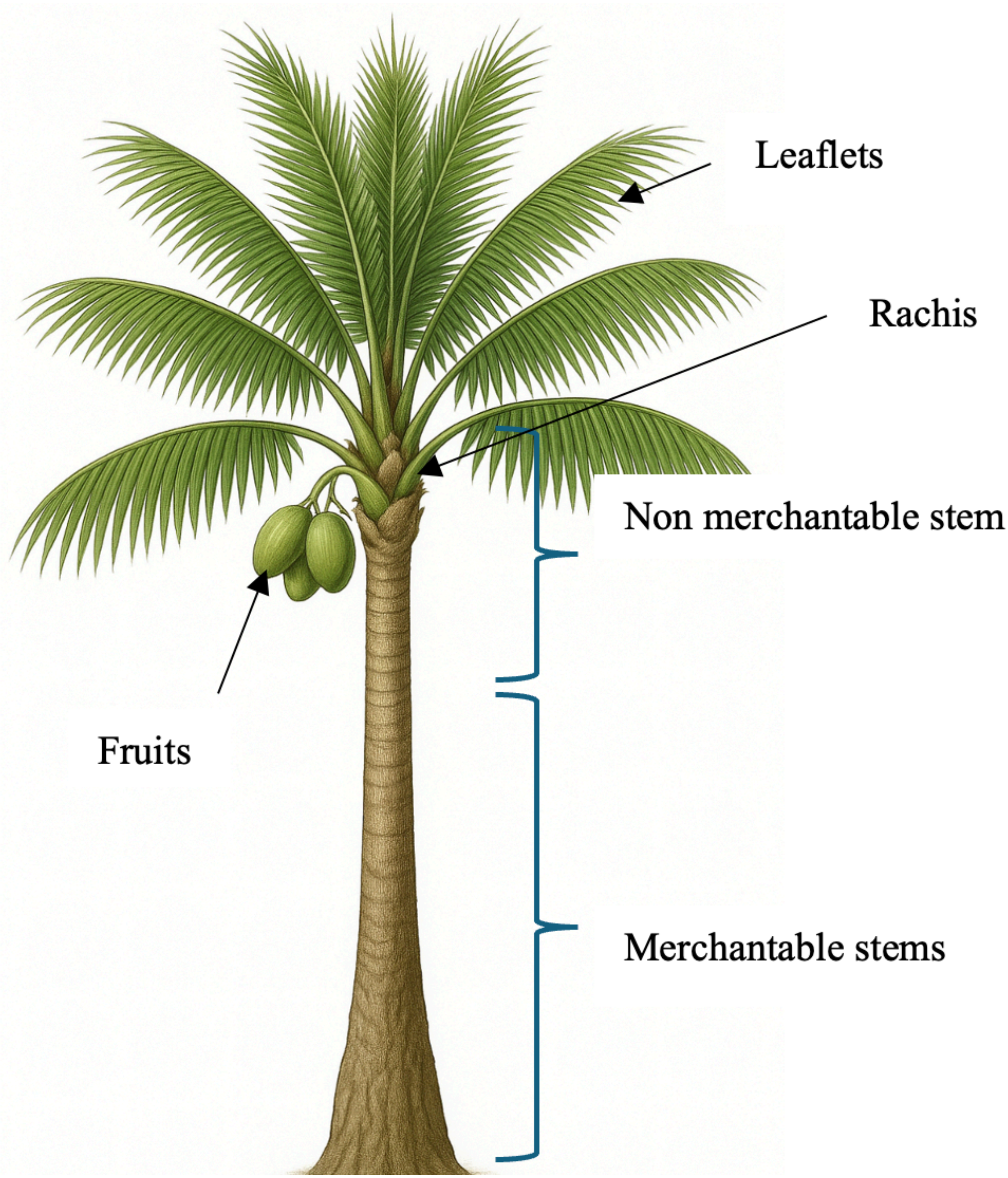

Figure 2

Aboveground component of the coconut palm

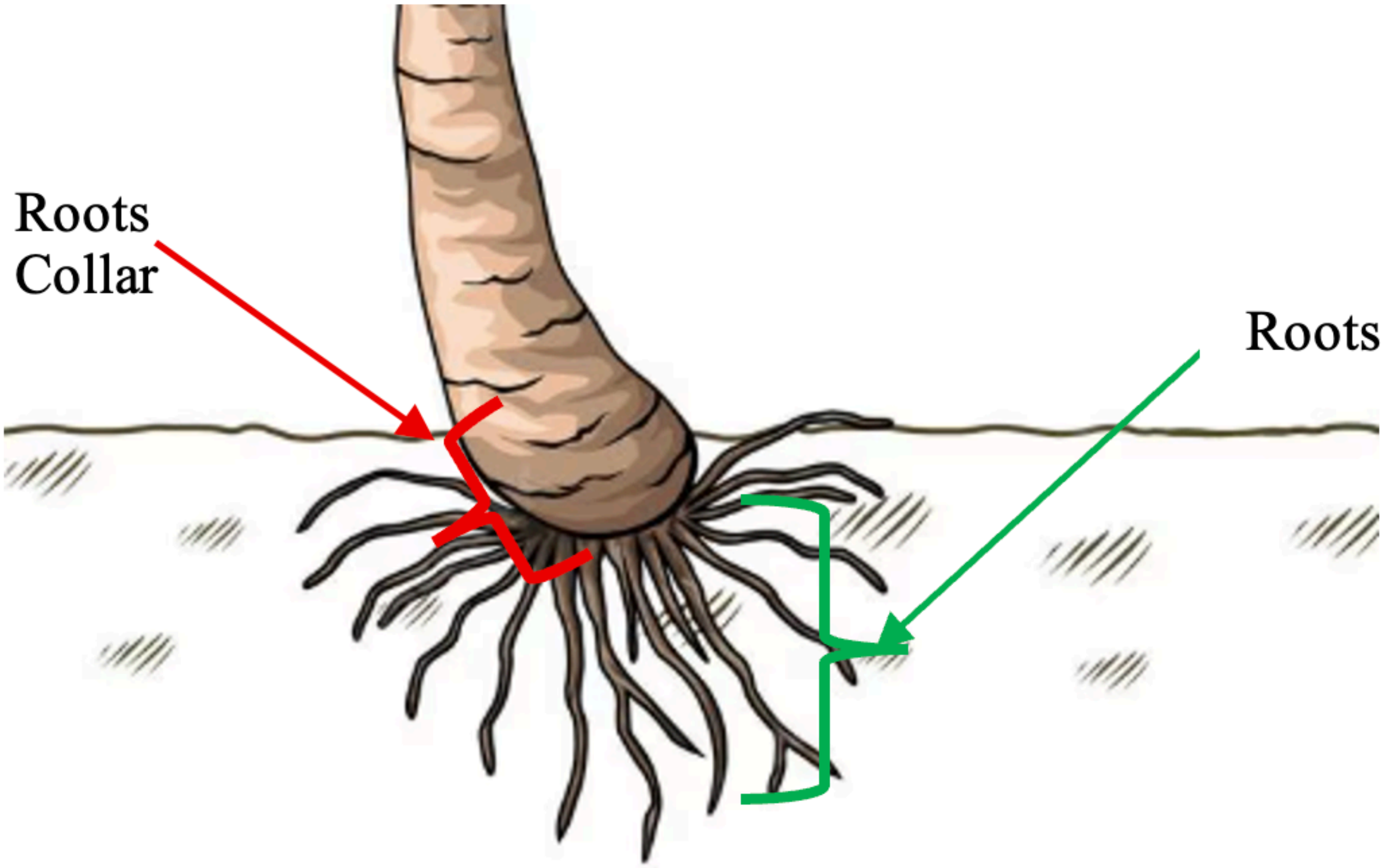

Figure 3

Components of the coconut tree

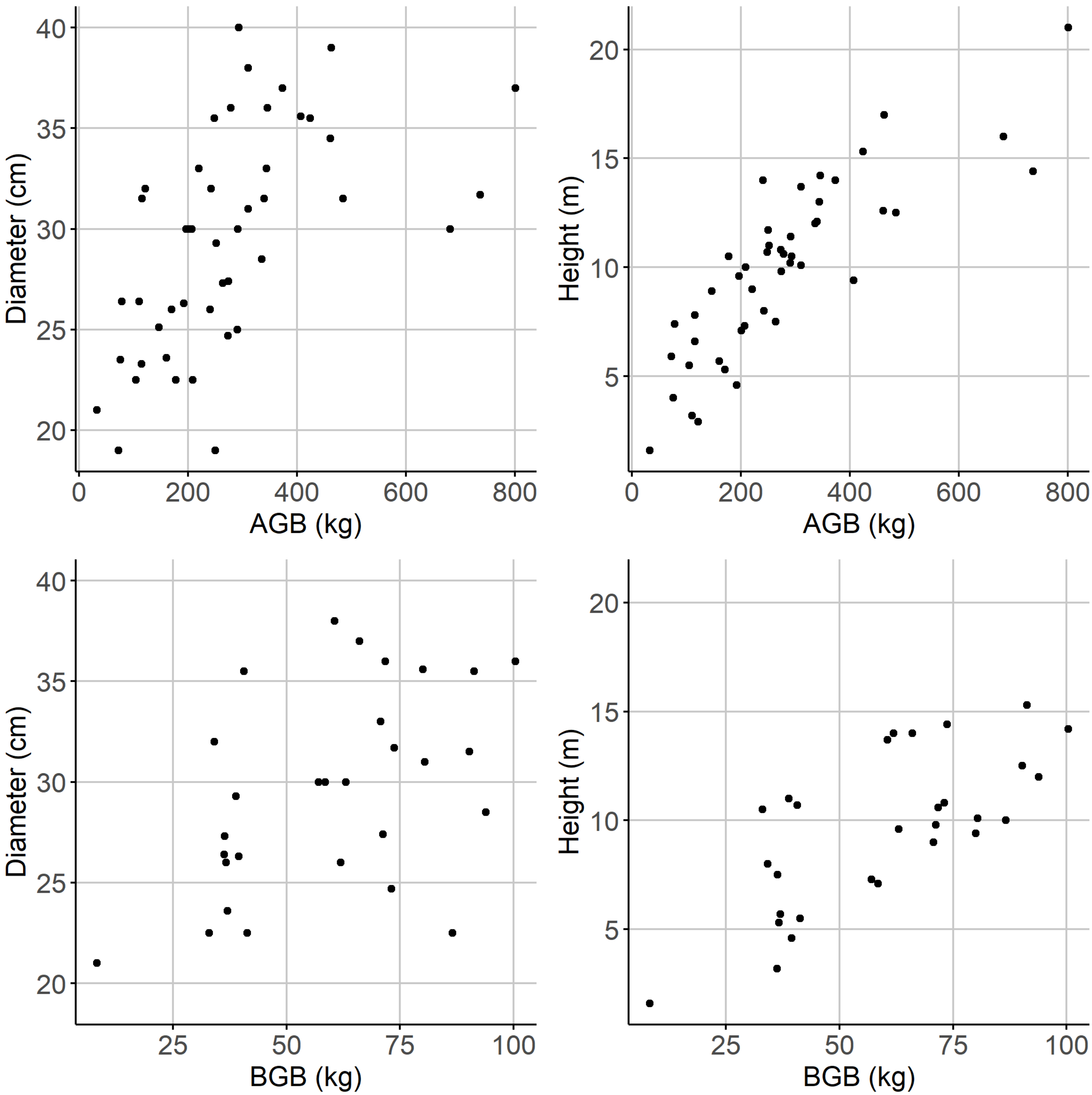

Figure 4

Scatter plots of AGB and BGB versus total H and D

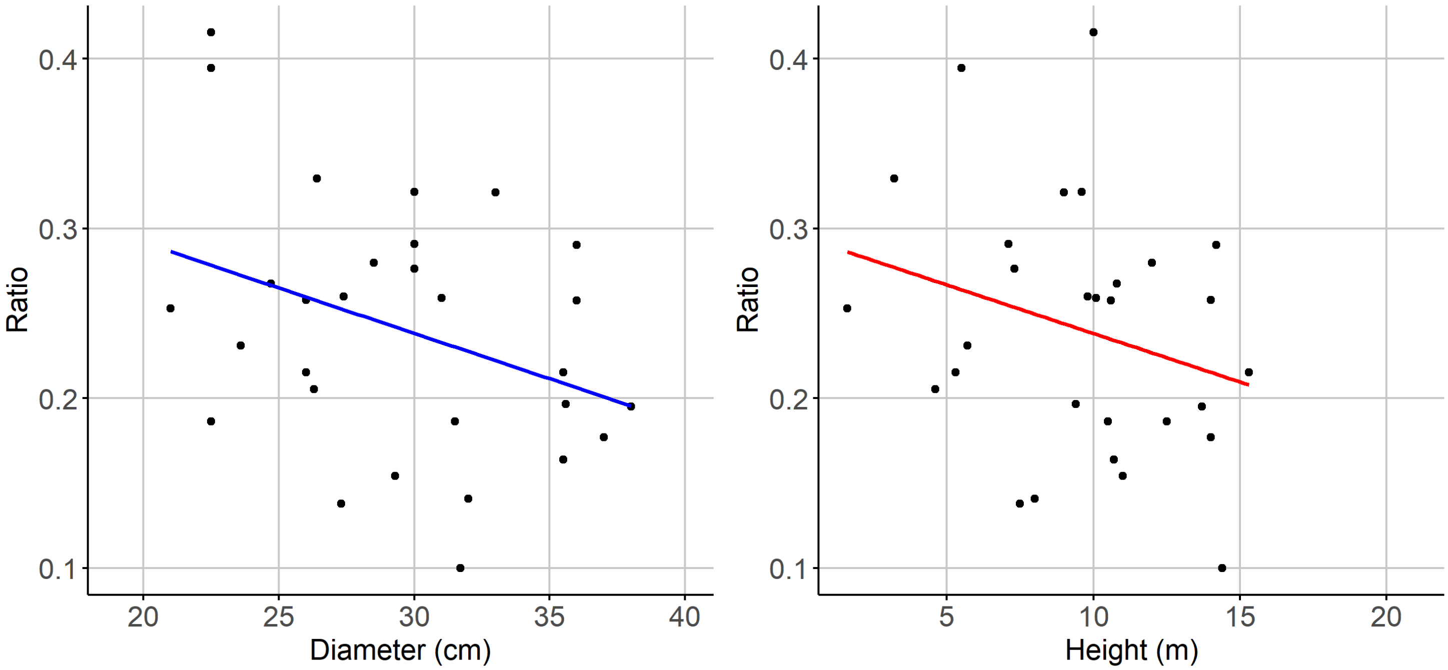

Figure 5

The root/shoot ratio versus D and H

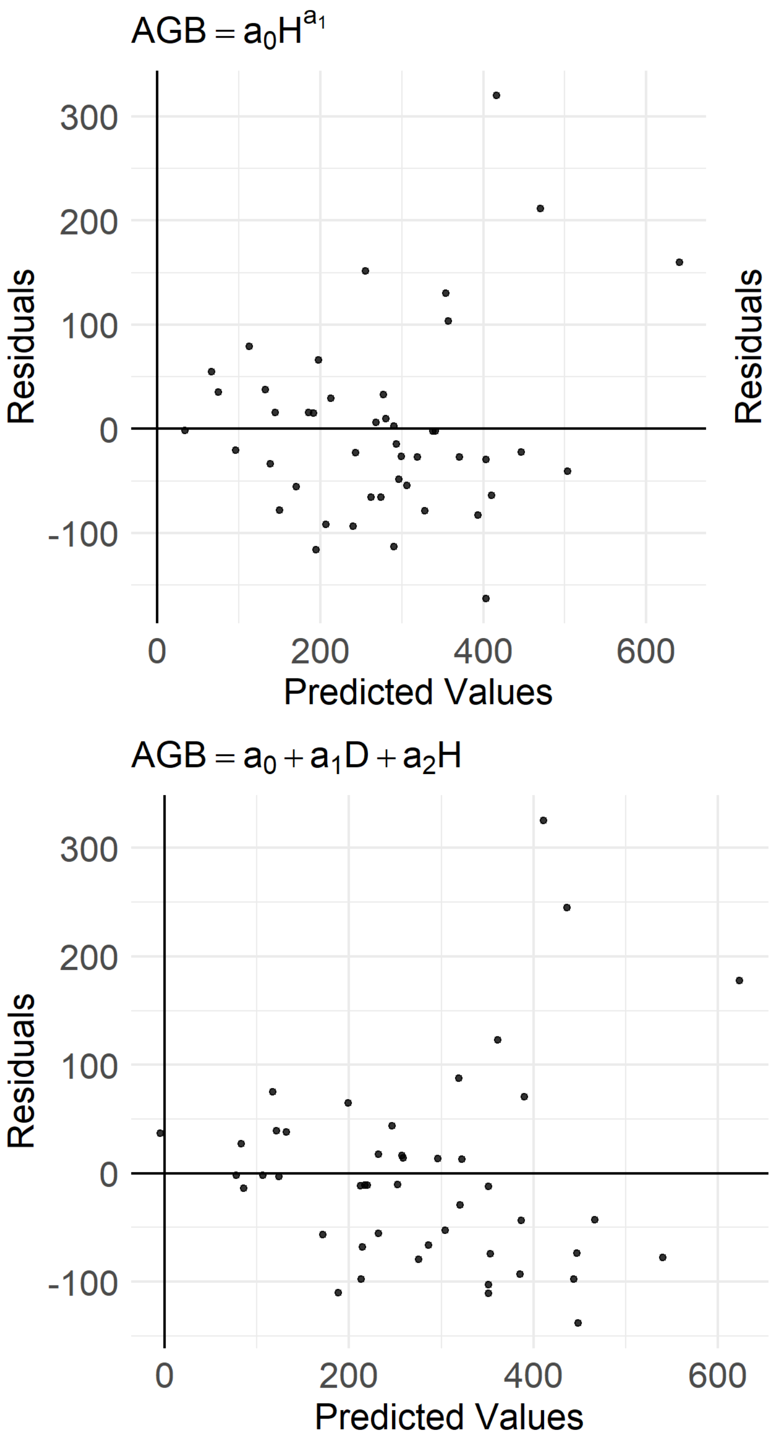

Figure 6

Residual plots of the selected AGB models

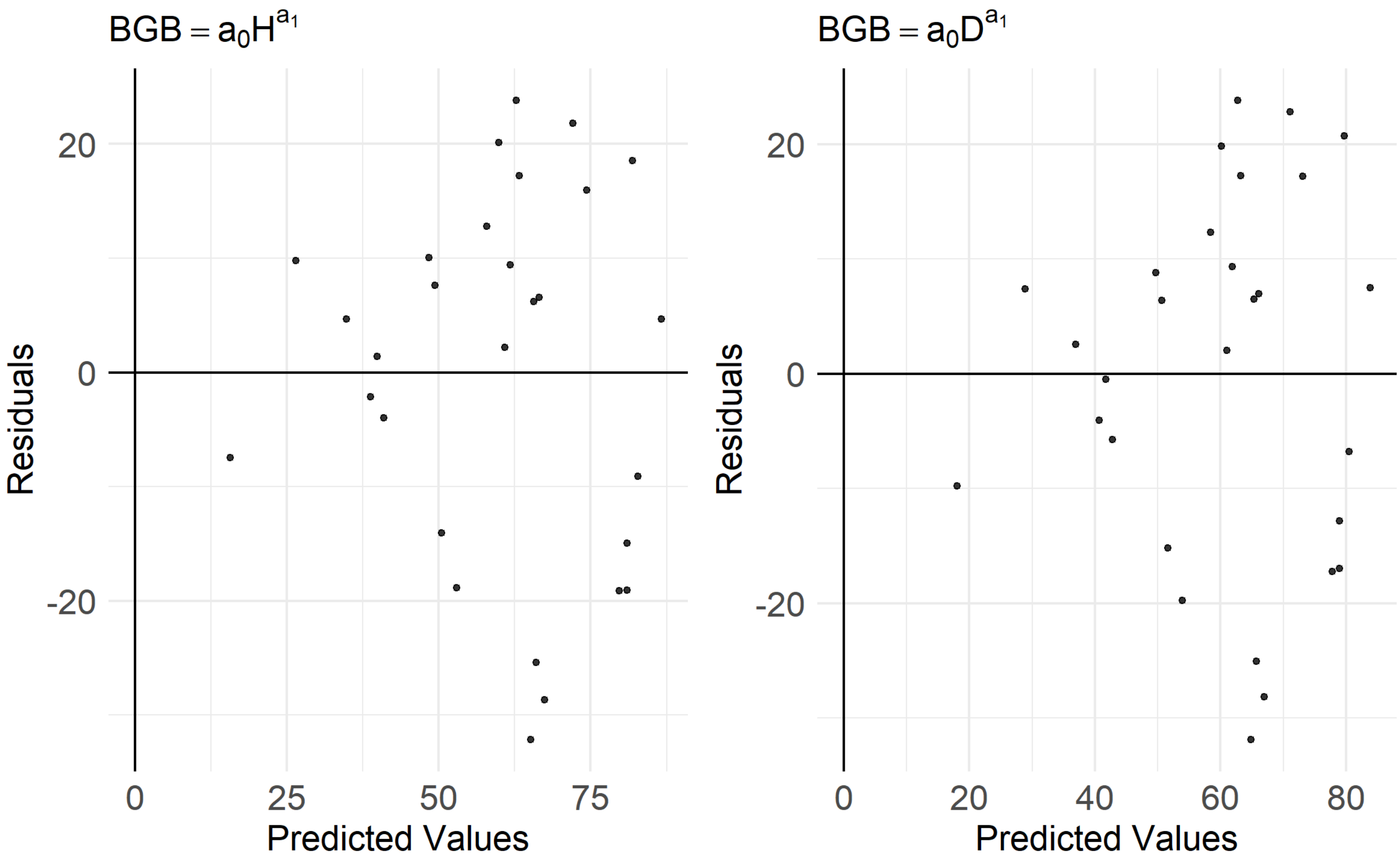

Figure 7

Residual plots of the selected BGB models